Electronic Supplementary Information (ESI)

Boosting Hydrogen Evolution via Flexoelectric Catalysis in gradient F-doped Hydroxyapatite Nanowires

Yucheng Zhang,[a] Jiawei Huang,[a] Lei Jiang,[b] Jun Qiang,[c] Zhouyang Zhang,[d] Zhanfeng Liu,[e] Yi Liu,[e] Tingfang Tian,*[a] Zhao Wang,*[b] and Linfeng Fei*[a]

[a] School of Physics and Materials Science, Jiangxi Provincial Key Laboratory of Photodetectors, Nanchang University, Nanchang, Jiangxi 330031, P.R. China

[b] Hubei Key Laboratory of Micro- & Nanoelectronic Materials and Devices, School of Microelectronics, Hubei University, Wuhan, Hubei 430062, P.R. China

[c] School of Mechanical Engineering, Ningxia University, Yinchuan, Ningxia 750021, P.R. China

[d] School of Materials and New Energy, Ningxia University, Yinchuan, Ningxia 750021, P.R. China

[e] National Synchrotron Radiation Laboratory, University of Science and Technology of China, Hefei, Anhui 230029, P.R. China

E-mail: feilinfeng@gmail.com (L. F. Fei); wangzhao@hubu.edu.cn (Z. Wang); tftian@ncu.edu.cn (T. F. Tian)

Contents of Supplementary Information:

Methods

Materials and reagents

All materials were used as received without further purification. Anhydrous calcium chloride ($CaCl_2$, AR ≥ 99%), anhydrous sodium dihydrogen phosphate (NaH_2PO_4, AR ≥ 99%), oleic acid ($C_{18}H_{34}O_2$, AR), sodium hydroxide (NaOH, AR ≥ 96%), and sodium fluoride (NaF, AR ≥ 99%) were purchased from Aladdin Reagent (Shanghai) Co., Ltd.

Synthesis of F-HAP NWs

F-HAP samples were synthesized by a modified hydrothermal method. Anhydrous $CaCl_2$ (4 mmol) and anhydrous NaH_2PO_4 (2.4 mmol) were dissolved in deionized water (8 ml), respectively. Then, the $CaCl_2$ solution was added dropwise into the NaH_2PO_4 solution. Subsequently, 16 ml of 0.7 M NaOH, 16 ml of oleic acid and 24 ml of ethanol were added to the above solution. After that, an appropriate amount of NaF (0 mmol, 0.4 mmol, 1.2 mmol, 2 mmol, or 2.8 mmol) was added to the mixture. The mixture was stirred and transferred to a 100 ml Teflon-lined autoclave and heated at 180 °C for 12 h. The product was first dispersed in alcohol and then collected by centrifugation at 8000 rpm for 5 min. The collected F-HAP NWs were then washed 3 times with ethanol. Besides, the synthesis of F-HAP NWs of different aspect ratios were performed according to Table S1 by changing the ratio of ethanol over water (η) in the hydrothermal reaction. All samples were calcined at 500 °C for 2 h before use.

Table S1 Synthesis of F-HAP NWs with varying aspect ratios.

Catalysts	$CaCl_2$ solution (ml)	NaH_2PO_4 solution (ml)	Oleic acid (ml)	Ethanol (ml)	NaOH solution (ml)	Ethanol: water (η)
S-HAP	12	12	16	16	16	4:10
M-HAP	10	10	16	20	16	5:9
L-HAP	8	8	16	24	16	6:8

General characterizations

XRD patterns were obtained on a Rigaku D/Max diffractometer with a Cu Kα radiation. SEM images were obtained on a Thermos Scientific Scios2 dual beam electron microscope operated at 20 kV. TEM experiments were conducted on a JEOL JEM-F200 cold-field-emission TEM operated at 200 kV, equipped with a dual silicon drift detectors (SDDs) EDS. HAADF-STEM images were obtained on a 300 kV double aberration-corrected Titan Themis Z electron microscope. UV-Vis DRS spectra were recorded on a Hitachi UH-4150 UV-Vis spectrophotometer with spectral-grade $BaSO_4$ as a reference. FTIR spectra were acquired using a Thermos Scientific Nicolet380 spectrometer. XPS spectra were collected on a Thermos Scientific ESCALAB Xi+ system. UPS measurements were performed at ARPES beamline (BL-13U) of National Synchrotron Radiation Laboratory (Hefei, China) with a DA30L analyzer. The energy and angular resolutions are better than 15 meV and 0.3°, respectively. The analysis chamber vacuum is better than 7×10^{-11} Torr at room temperature.

PFM test

PFM test was performed on a NT-MDT scanning probe microscope (SPM, NT-MDT Ntegra upright). By moving the probe tip of PFM to the middle region of the scanned NW, the displacement-voltage butterfly curve and the phase curve with 180° flip of the phase were obtained upon applying a voltage.

Finite element simulations

Finite element method was performed by the COMSOL software. The diameter of the F-HAP NWs was set to 50 nm, and the length was set to 300, 600, or 1000 nm. The elastic modulus and Poisson's ratio of the F-HAP NWs were set to 30.83 GPa and 2.03, respectively. The NW was simply supported at both ends, and an axial displacement

constraint was set at the bottom to ensure that the NW could bend freely. The bending of the NW was realized by applying bending moments at both ends. The bending moment was set to 10^{-12} N·m to approximate the level of strain gradient in our experiments.

Hydrogen evolution test

Hydrogen evolution test was typically performed by dispersing 50 mg of F-HAP NWs into 50 ml of deionized water in a homemade reactor (150 ml). Before the test, the system was blown by a flow of Ar for 30 min. The evolved H_2 was quantitatively analyzed by a gas chromatograph (Shimadzu GC-2014) with Ar as the carrier gas.

Supplementary Figures

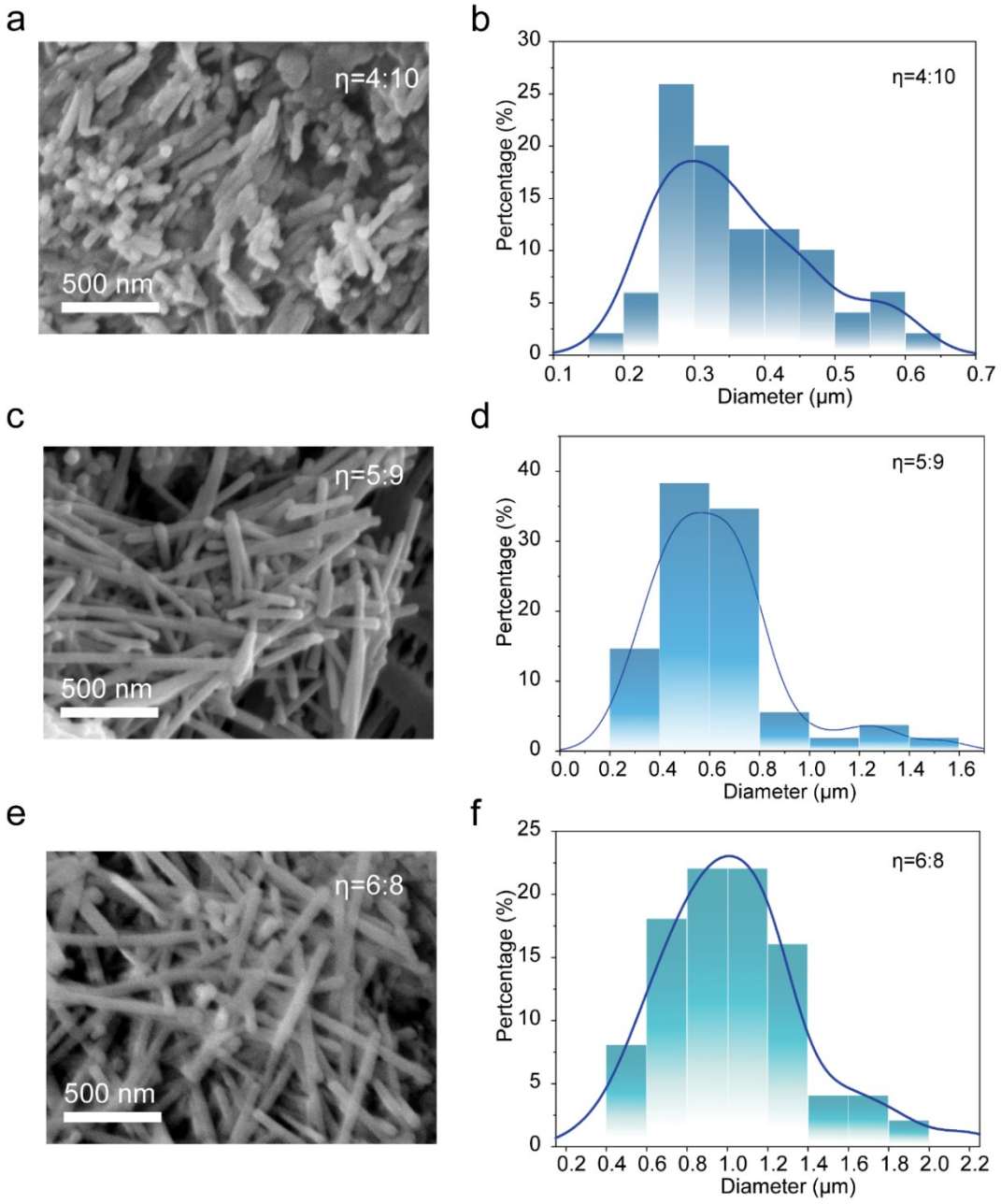

Figure S1 Statistics of lengths and diameters for HAP NWs. (a, b) Length statistics of S-HAP NWs (η=4:10). (c, d) Length statistics of M-HAP NWs (η=5:9). (e, f) Length statistics of L-HAP NWs (η=6:8).

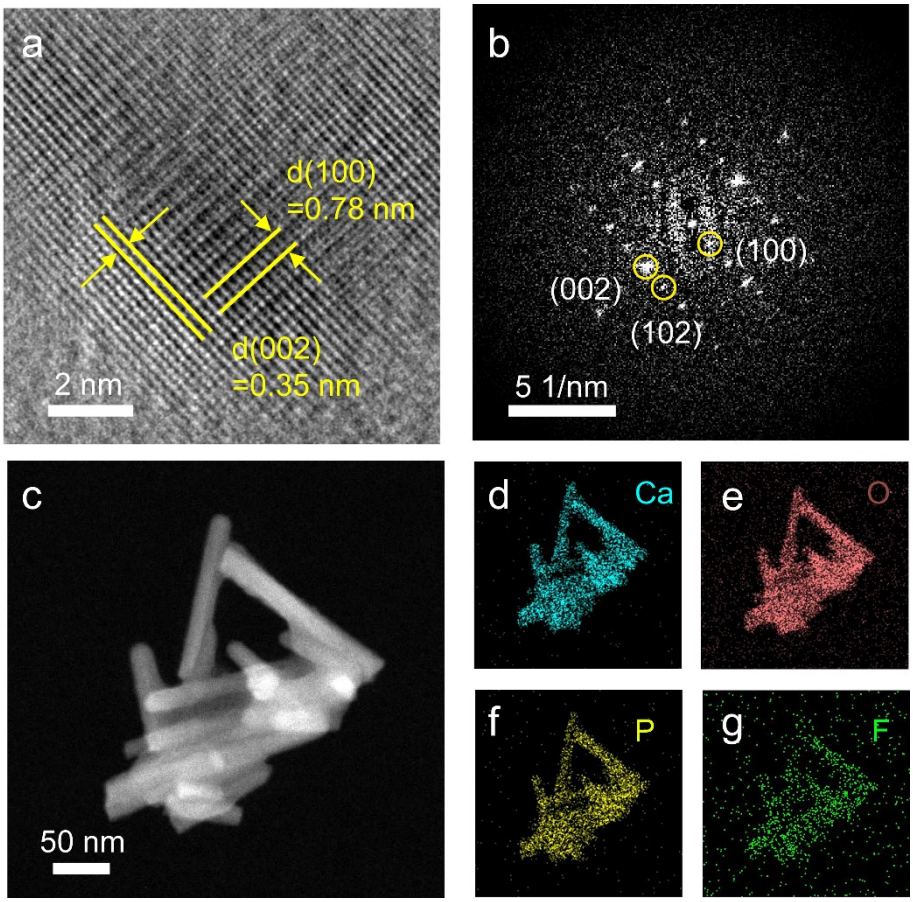

Figure S2 Morphological characterization and elemental distributions of F-HAP NWs. (a) HRTEM image of a NW. (b) FFT pattern. (c) HAADF-STEM image and (d-g) the EDS elemental mappings for Ca, O, P, and F.

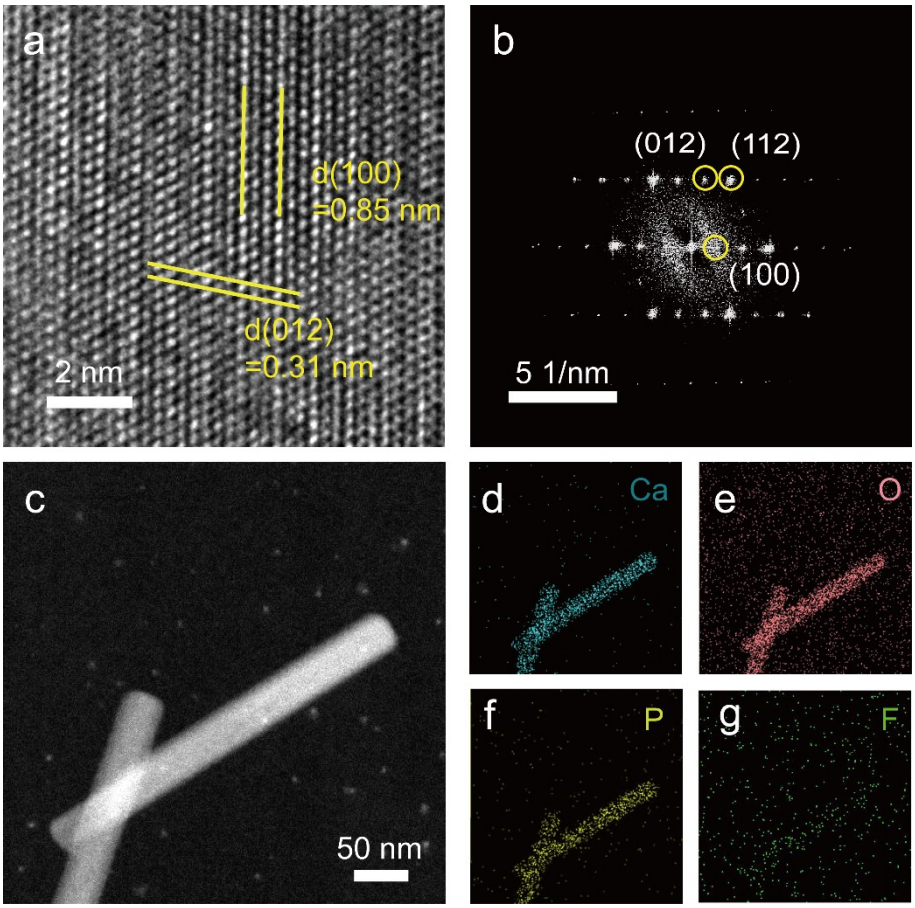

Figure S3 Morphological characterization and elemental distributions of HAP NWs. (a) HRTEM image of a NW. (b) FFT pattern. (c) HAADF-STEM image and (d-g) the EDS elemental mappings for Ca, O, P, and F.

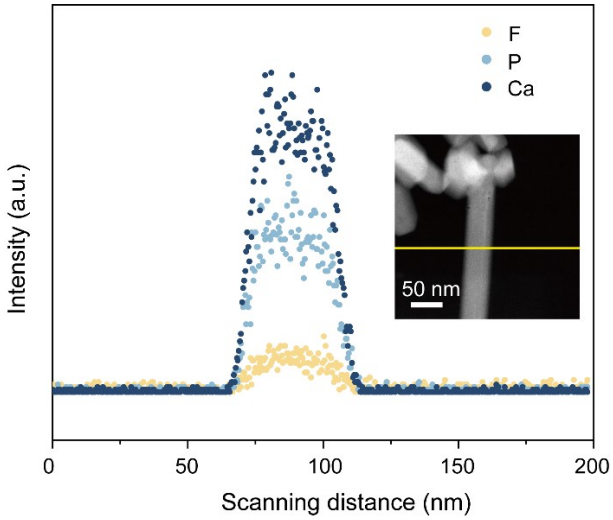

Figure S4 EDS line scan for F, P and Ca elements in an F(5)-HAP NW.

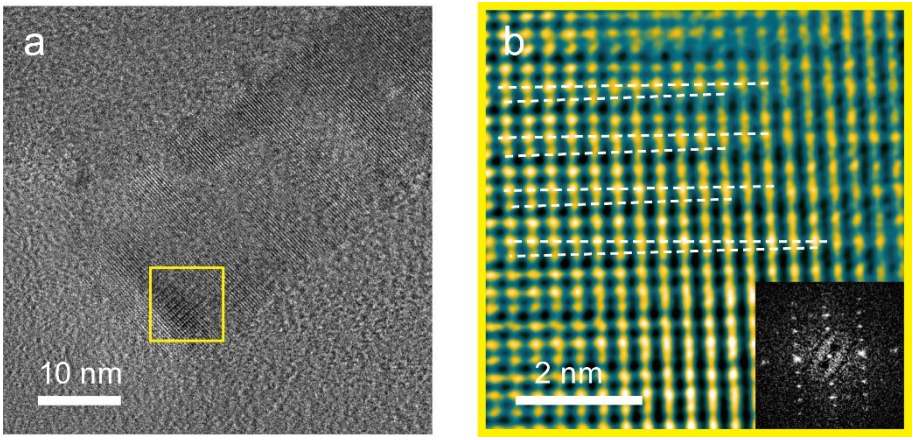

Figure S5 Lattice-resolved HRTEM image of an F(5)-HAP NW. (a) HRTEM image. (b) The observation of lattice distortions after gradient F-doping.

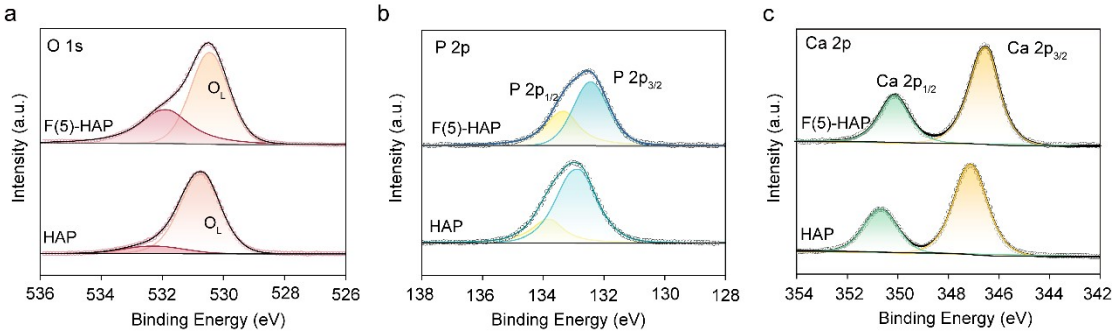

Figure S6 High-resolution XPS spectra of (a) O 1s, (b) P 2p, and (c) Ca 2p for F(5)-HAP and HAP NWs.

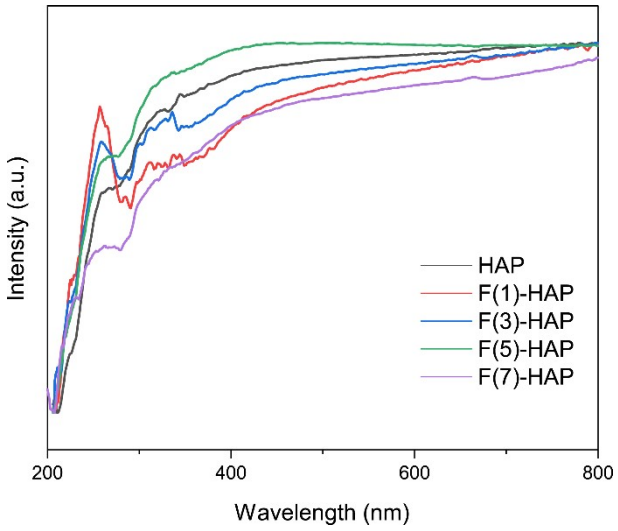

Figure S7 UV profiles of HAP, F(1)-HAP, F(3)-HAP, F(5)-HAP and F(7)-HAP NWs.

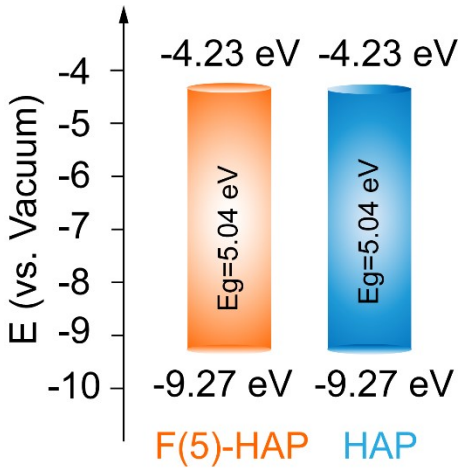

Figure S8 Comparison of optical bandgaps for HAP and F(5)-HAP NWs.

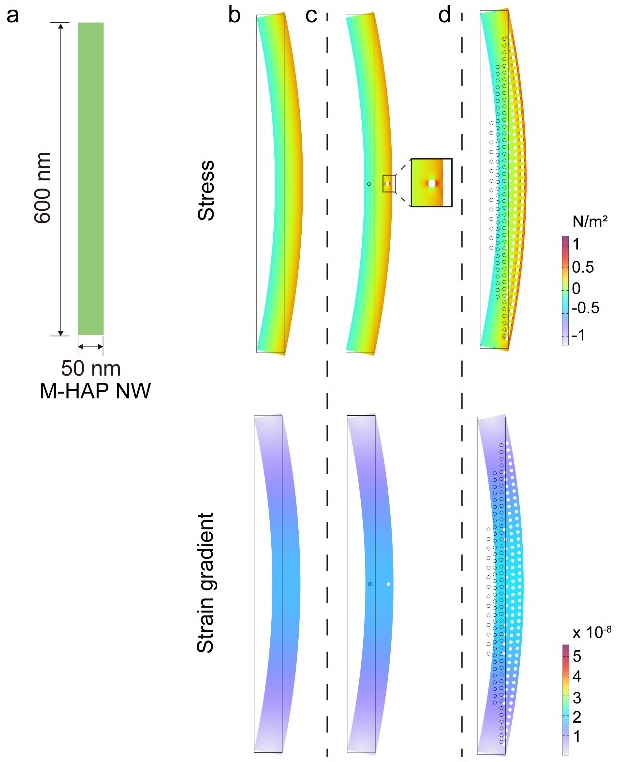

Figure S9 (a) A single M-HAP NW model for FEM. (b) FEM results for bending induced stress and strain distributions within the NW. (c) FEM results for bending induced stress and strain gradient upon doped with one atom within the NW. (d) FEM results for bending induced stress and strain gradient upon surface doping within the NW.

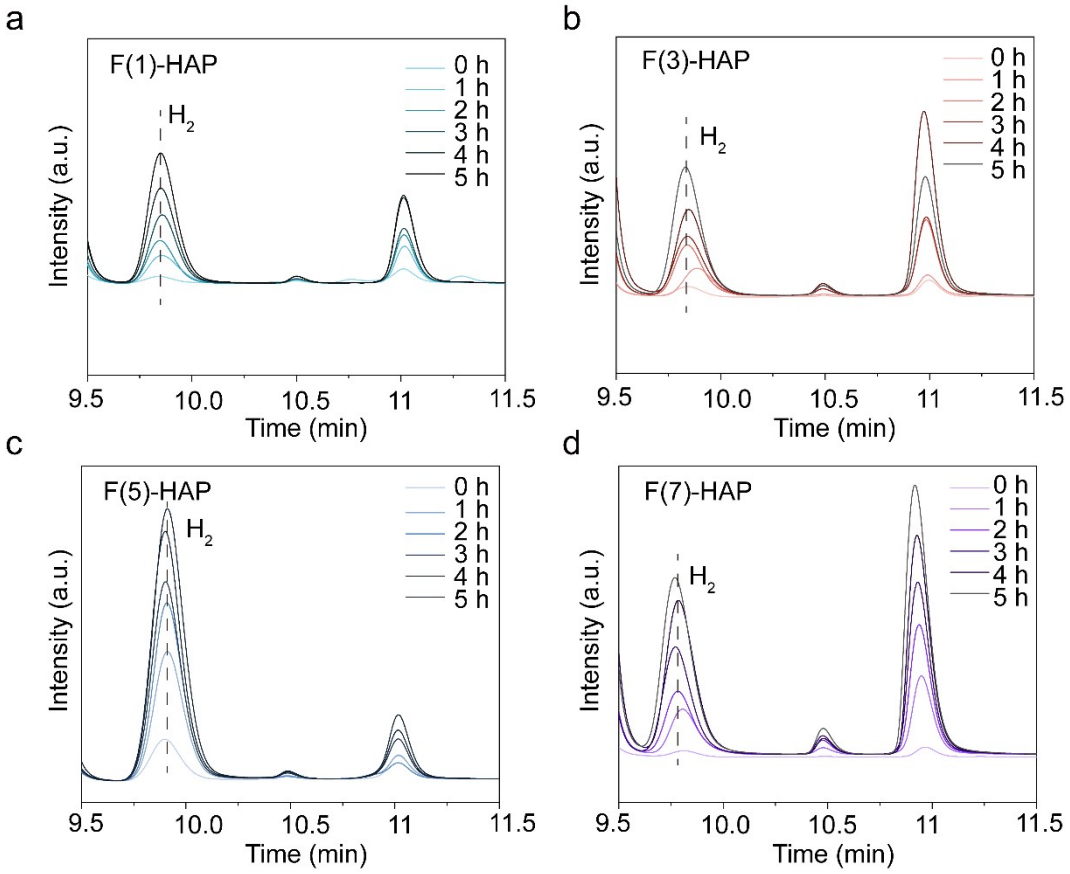

Figure S10 GC data for hydrogen gas productions of (a) F(1)-HAP NWs, (b) F(3)-HAP NWs, (c) F(5)-HAP NWs, and (d) F(7)-HAP NWs.

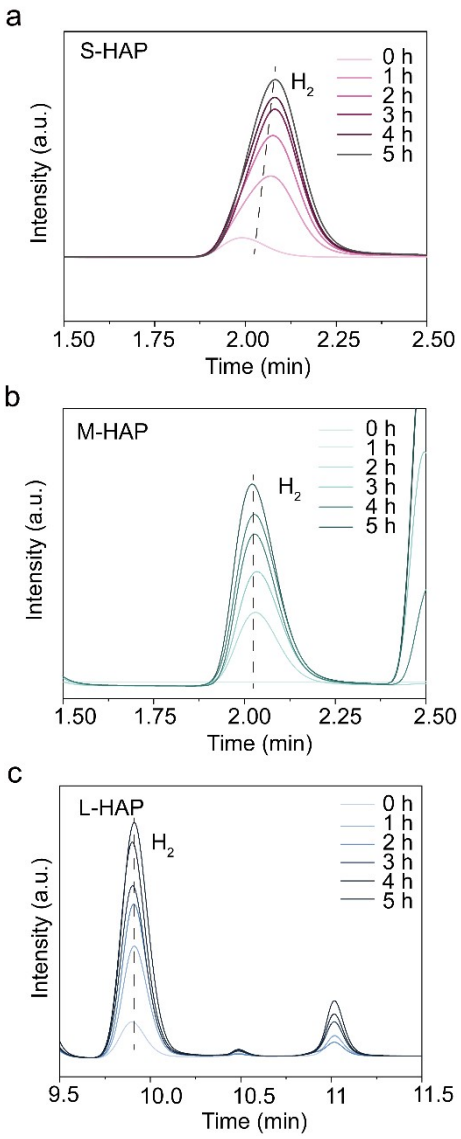

Figure S11 GC data for hydrogen gas productions of (a) S-HAP NWs, (b) M-HAP NWs, and (c) L-HAP NWs.

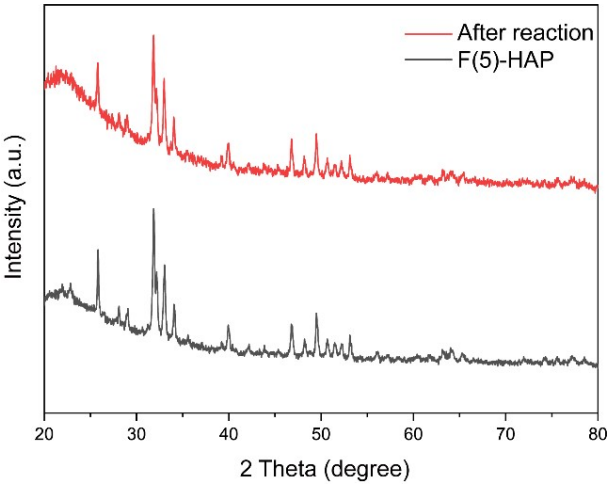

Figure S12 XRD patterns for F(5)-HAP NWs before and after catalytic reaction.

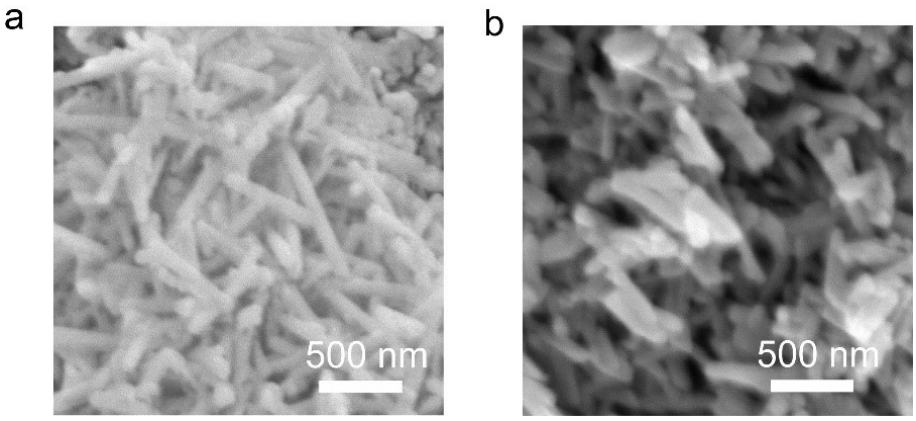

Figure S13 (a) SEM of F(5)-HAP NWs. (b) SEM of F(5)-HAP NWs after three catalytic cycles.

Table S2 Typical catalysts and their performance in hydrogen evolution reaction.

Catalyst	Precious metal	Catalytic Mechanism	Activity [H_2 μmol g^{-1} h^{-1}]	Year [Reference]
F-HAP NWs	---	Flexo-	322.7	This work
$MoSe_2$	---	Piezo-Flexo-	4858.2	2020[1]
S-Pt/CN	Pt	Piezo-Flexo-	1283	2023[2]
CNF700	Pt	Photo-Flexo-	11900	2023[3]
Ag(CuZn)(AlCr)	Ag	Flexo-	1716	2023[4]
TiO_2 nanosheets	---	Flexo-	308.5	2024[5]
TiO_2 (Rutile)	---	Flexo-	1830	2024[6]
CeO_2 nanorods	---	Flexo-	486.4	2024[7]

References

1. Y. J. Chung, C. S. Yang, J. T. Lee, G. H. Wu and J. M. Wu, Coupling effect of piezo–flexocatalytic hydrogen evolution with hybrid 1T- and 2H-phase few-layered $MoSe_2$ nanosheets, *Adv. Energy Mater.*, 2020, **10**, 2002082.
2. Y. T. Wang, H. Y. Lin, Y. C. Chen, Y. G. Lin and J. M. Wu, Piezo-flexocatalysis of single-atom Pt-loaded graphitic carbon nitride, *Small Methods*, 2023, **8**, 2301287.
3. H. Tan, W. Si, W. Peng, X. Chen, X. Liu, Y. You, L. Wang, F. Hou and J. Liang, Flexo-/piezoelectric polarization boosting exciton dissociation in curved two-dimensional carbon nitride photocatalyst, *Nano Lett.*, 2023, **23**, 10571-10578.
4. P. Y. Wu, K. T. Le, H. Y. Lin, Y. C. Chen, P. H. Wu and J. M. Wu, Flexoelectric catalysts based on hierarchical wrinkling surface of centrosymmetric high-entropy oxide, *ACS Nano*, 2023, **17**, 17417-17426.
5. Y. C. Chen, P. H. Chen, Y. S. Liao, J. P. Chou and J. M. Wu, Defect engineering centrosymmetric 2D material flexocatalysts, *Small*, 2024, **20**, 2401116.
6. Y. Du, S. Zhang and Z. Cheng, Flexocatalysis of nanoscale titanium dioxide, *Nano Energy*, 2024, **127**, 109731.
7. L. Sai, Y. Xiao, F. Yan, T. Ying, Z. Wu, H. Xu, Y. Jia and F. Wang, Integration of hydrogen evolution and dye removal in flexocatalysis by centrosymmetric semiconductor nanorods, *Int. J. Hydrogen Energy*, 2024, **69**, 944-952.